Inspection of new physics in $B_s \to K^+K^-$ decay mode

Manas K. Mohapatra*
Department of Physics, IIT Hyderabad, Kandi -502285, India

(Received 5 November 2019; accepted 11 March 2020; published 16 April 2020)

We scrutinize the penguin dominated $B_s \to K^+K^-$ decay mode involving $b \to s$ quark level transition in family nonuniversal Z' and vectorlike down quark model. There is discrepancy in the standard model branching ratio value of this mode with the experimental results reported by Belle, CDF, and LHCb Collaborations. Additionally, the measured values of CP-violating asymmetries $C_{K^+K^-}$ and $S_{K^+K^-}$ deviate from the SM predictions. We constrain the new parameter space by using the existing experimental limits on leptonic $B_s \to \ell\ell$ ($\ell = e, \mu, \tau$) processes. We then check the effects of new physics on the branching ratio and CP-violating parameters of the $B_s \to K^+K^-$ process.

DOI: 10.1103/PhysRevD.101.075033

I. INTRODUCTION

The in-depth search for physics beyond the standard model (SM) plays an important role in the area of particle physics. It is known that the CP asymmetry, the symmetry violation of combination of charge conjugation (C) and parity (P), is the main source for matter-antimatter asymmetry that is observed in our present universe. In the sector of quarks, the Cabbibo-Kobayasi-Maskawa (CKM) matrix indicates a message for an insight to the gateway of CP violation, particularly in B and K meson decays in the SM. However, it is not sufficient to understand the observed baryon asymmetry. Recently, various experimental hunts are going on to probe the physics beyond the SM. In this regard, B meson system provides an important role to study prominent observables like branching ratio and CP-violating parameters such as direct and mixing-induced CP asymmetry to probe new physics.

We would like to study the $b \to s$ penguin dominated $B_s \to K^+K^-$ decay mode which appears to have discrepancies in standard model values of CP-averaged branching ratio and CP-violating parameters with the corresponding observed values. The theoretical result for the observables is given in Table I. Additionally, Table II shows the results from Belle, CDF, and LHCb Collaborations along with world averages. Thus, these discrepancies between observed and predicted results could lead to probe the physics beyond the SM.

In addition to this, the leptonic decays of pseudoscalar B_s meson sector plays a vital role and enthusiastically makes more attention to explore the physics beyond the SM. In particular, we study $B_s \to \mu^+\mu^-$ decay mode because of careful observation of decay constant of neutral B_s^0 meson from lattice. On the other side, the study of $B_s \to \ell'\ell'$ (where $\ell' = e, \tau$) puts a less mark on the board as they have upper bounds. The former one has branching ratio with an upper limit of 2.8×10^{-7} (90% C.L.) [12], reported by LHCb where $< 6.8 \times 10^{-3}$ (95% C.L.) reported by CDF Collaboration [13] for later decay mode. The SM values of branching ratio of $B_s \to \tau^+\tau^-$ and $B_s \to e^+e^-$ decays have $\mathcal{O}(10^{-7})$ and $\mathcal{O}(10^{-14})$, respectively, where as for $B_s \to \mu^+\mu^-$, it is of the order of 10^{-9} [14]. Thus, there is a possibility of contribution to both decays along with $B_s \to \mu^+\mu^-$ mode in the new physics scenario.

Inspired by these discrepancies of the $B_s \to K^+K^-$ decay mode, we would like to investigate, in QCD factorization approach, the new physics (NP) effect on CP-averaged branching ratio as well as the CP violation parameters arising due to Z' model where an extra $U(1)'$ gauge boson Z' takes part in the play. Several studies

TABLE I. The theoretical predictions of CP-averaged branching ratio ($\mathcal{B}$) (in the units of 10^{-6}), CP-violating asymmetries such as direct (C_{KK} in %) and mixing-induced CP asymmetry (S_{KK}).

$B_s \to K^+K^-$	QCDF [1]	PQCD [2,3]	SCET [4]
$\mathcal{BR}$	$25.2\ ^{+12.7+12.5}_{-7.2-9.1}$	13.6 $19.7\ ^{+6.6}_{-5.7}$	18.2
$\mathcal{C}_{\rm KK}$	$-7.7\ ^{+1.6+4.0}_{-1.2-5.1}$	−23.3 −16.4	−6
$\mathcal{S}_{\rm KK}$	$0.22^{+0.04+0.05}_{-0.05-0.03}$	28 20.6	19

*manasmohapatra12@gmail.com

TABLE II. Measured values of branching ratio ($\mathcal{B}$) (in the units of 10^{-6}), CP-violating asymmetries such as direct (C_{KK}) and mixing-induced (S_{KK}) reported by Belle, CDF, and LHCb Collaborations and world averages.

$\bar{B}_s \to K^+K^-$	Belle [5]	CDF [6]	LHCb [7–9]	HFLAV [10]	PDG [11]
$\mathcal{BR}$	$38^{+10}_{-09} \pm 7$	$23.9 \pm 1.4 \pm 3.6$	$23.0 \pm 0.7 \pm 2.3$	24.8 ± 1.7	25.9 ± 1.7
$\mathcal{C}_{KK}$	…	…	$0.14 \pm 0.11 \pm 0.03$ $0.20 \pm 0.06 \pm 0.02$	…	0.14 ± 0.11
$\mathcal{S}_{KK}$	…	…	$0.30 \pm 0.12 \pm 0.04$ $0.18 \pm 0.06 \pm 0.02$	…	0.30 ± 0.13

[15–18] have been done in the scenario of FCNC mediated by Z' boson. In addition to this, we study the new physics impact due to vectorlike down quark (VLDQ) model [18–21] where an extra $SU(2)_L$ singlet down type quark has been added to SM quark sector which includes a CP and flavor-violating FCNC mediated by Z boson at tree level. The new coupling $Z' - b - s$ ($Z - b - s$) associated with Z' (VLDQ) model can be constrained by using the experimental limit for all leptonic modes, and using the allowed parameter space, we examine the new physics impact on $B_s \to K^+K^-$ decay mode observables.

The layout of this paper is structured as follows. In Sec. II, we discuss the effective Hamiltonian responsible for the nonleptonic $b \to sq\bar{q}$ processes. We have also presented the framework for $B_s \to K^+K^-$ observables such as branching ratio and CP-violating parameters in the standard model. We constrain the new parameter space arising due to Z' model from the branching ratios of leptonic B_s modes in Sec. III and address the footprint of this model on $B_s \to K^+K^-$ process by using the new couplings. In Sec. IV, we draw an attention to the interactions of the VLDQ model and check the impact on the aforementioned observables for $B_s \to K^+K^-$ decay mode. Section V summarizes our results.

II. $B_s \to K^+K^-$ PROCESS IN THE STANDARD MODEL

In the standard model, the penguin dominated $B_s \to K^+K^-$ decay mode receives contribution from quark level transition $b \to s$ where the weak effective Hamiltonian describing the decay $b \to sq\bar{q}$ is given as [22]

$$\mathcal{H}_{\rm eff} = \frac{G_F}{\sqrt{2}}\left\{V_{ub}V_{us}^*[C_1(\mu)O_1^u(\mu) + C_2(\mu)O_2^u(\mu)] - V_{tb}V_{ts}^*\left[\sum_{i=3}^{10} C_i(\mu)O_i(\mu)\right]\right\} + \text{H.c.}, \quad (1)$$

where $G_F = 1.16639 \times 10^{-5}$ GeV^{-2} is the Fermi coupling constant, $V_{\alpha\beta}$'s are the CKM matrix element ($\alpha, \beta = u, b, s, t$). Here $O_{1,2}$ are the current-current operators, $O_{3,\ldots 6}$ are QCD penguin operators, $O_{7,\ldots 10}$ are electroweak penguin operators, and $C_i(\mu)$ ($i = 1, \ldots 10$) are the corresponding Wilson coefficients evaluated at the renormalization scale $\mu = m_b$.

Using the framework of QCD factorization approach [23], the decay amplitude can be written in the form as

$$\langle K^+K^-|O_i|B_s^0\rangle = \langle K^+K^-|O_i|B_s^0\rangle_{\rm fact} \times \left[1 + \sum r_n \alpha_s^n + O\left(\frac{\Lambda_{\rm QCD}}{m_b}\right)\right], \quad (2)$$

where $\langle K^+K^-|O_i|B_s^0\rangle_{\rm fact}$ represents the hadronic factorized matrix element, the second and third terms in the square bracket are higher order corrections. The coupling constant α_s arises due to strong interaction effect, $\Lambda_{\rm QCD}$ is the QCD scale.

In the heavy quark limit, the amplitude of this decay mode can be represented as [23]

$$\mathcal{A}_{B_s^0\to K^+K^-} = A_{K\bar{K}}[\delta_{pu}\alpha_1 + \alpha_4^p + \alpha_{4,EW}^p + \beta_3^p + \beta_4^p - \frac{1}{2}\beta_{3,EW}^p - \frac{1}{2}\beta_{4,EW}^p] + B_{\bar{K}K}[\delta_{pu}b_1 + b_4^p + b_{4,EW}^p], \quad (3)$$

where

$$A_{K\bar{K}} = i\frac{G_F}{\sqrt{2}}m_B^2 F_0^{B_s\to K}(0) f_K,$$
$$B_{\bar{K}K} = i\frac{G_F}{\sqrt{2}} f_{B_s} f_K f_K, \quad (4)$$

which includes the form factor $F_0^{B_s\to K}(0)$ at zero recoil momentum and decay constants f_{B_s} and f_K. The detailed expressions of coefficients α_i and β_i (b_i) are given in the Appendix, which include factorizable along with non-factorizable contributions to the above decay amplitude.

The CP-averaged branching ratio can be obtained using the following formula:

$$\mathcal{BR}(B_s \to K^+K^-) = \tau_{B_s}\frac{p_c}{8\pi m_{B_s}^2}\left[\frac{|\mathcal{A}_{B_s\to K^+K^-}|^2 + |\mathcal{A}_{\bar{B}_s\to K^+K^-}|^2}{2}\right], \quad (5)$$

where τ_{B_s} (m_{B_s}) is the lifetime (mass) of B_s meson and the center of mass momentum in the rest frame of B meson is given as

$$p_c = \sqrt{(m_{B_s}^2 - (m_{K^+} + m_{K^-})^2)(m_{B_s}^2 - (m_{K^+} - m_{K^-})^2)}. \quad (6)$$

The amplitudes correspond to B_s and $\bar{B}_s$ are CP conjugate to each other. The time-dependent CP asymmetry of B_s meson decaying to final CP eigenstate K^+K^- can be written as [24]

$$\mathcal{A}_{K^+K^-}(t) = C_{KK}\cos(\Delta M_{B_s^0} t) + S_{KK}\sin(\Delta M_{B_s^0} t), \quad (7)$$

where $C_{KK} = \frac{|\lambda|^2-1}{1+|\lambda|^2}$ and $S_{KK} = 2\frac{\mathrm{Im}(\lambda)}{1+|\lambda|^2}$ are the direct and the mixing-induced CP asymmetries, respectively [1]. The parameter λ is given as

$$\lambda = \frac{q}{p}\frac{\mathcal{A}_{\bar{B}_s^0\to K^+K^-}}{\mathcal{A}_{B_s^0\to K^+K^-}}, \quad (8)$$

where q and p are mixing parameters which are connected to the standard model CKM elements as

$$\frac{q}{p} = \frac{V_{tb}^* V_{ts}}{V_{tb}V_{ts}^*}. \quad (9)$$

Symbolically, the amplitude of the $B_s \to K^+K^-$ decay mode can be written as

$$\mathcal{A}_{B_s^0\to K^+K^-} = \zeta_u \mathcal{A}_u + \zeta_c \mathcal{A}_c = \zeta_c \mathcal{A}_c[1 + \wp a e^{i(\delta_1-\gamma)}], \quad (10)$$

where $\zeta_q = V_{qb}V_{qs}^*(q = u, c)$, $a = |\frac{\zeta_u}{\zeta_c}|$, $\wp = |\frac{\mathcal{A}_u}{\mathcal{A}_c}|$, γ is the weak phase of CKM element V_{ub}, and $\delta_1 = \mathrm{Arg}(\frac{\mathcal{A}_u}{\mathcal{A}_c})$. From the amplitude given in Eq. (10), the parameters $\mathcal{BR}$, $\mathcal{C}_{KK}$, and $\mathcal{S}_{KK}$ can be obtained, respectively, as

$$\mathcal{BR} = \frac{\tau_{B_s} p_c}{8\pi m_{B_s}^2}|\zeta_c \mathcal{A}_c|^2\{1 + (\wp a)^2 + 2\wp a\cos\delta_1\cos\gamma\}, \quad (11)$$

$$\mathcal{C}_{KK} = -\frac{2\wp a \sin\delta_1 \sin\gamma}{1 + (\wp a)^2 + 2\wp a\cos\delta_1\cos\gamma}, \quad (12)$$

$$\mathcal{S}_{KK} = \frac{\sin 2\beta + 2\wp a\cos\delta_1 \sin(2\beta-\gamma) + (\wp a)^2\sin(2\beta - 2\gamma)}{1 + (\wp a)^2 + 2\wp a\cos\delta_1\cos\gamma}. \quad (13)$$

For numerical computation of these observables in the SM, the CKM matrix elements along with the weak angle γ and the lifetime of B_s meson are taken from [11] and we use the value of β_s angle from [25]. The Wilson coefficients in NDR scheme at NLO correspond to flavor (α_i) and annihilation (β_i) contributions are considered from [26]. In addition to this, we use the values of other parameters which are given as follows:

(i) QCD scale and running quark masses

$$\Lambda_{\bar{MS}}^{(5)} = 0.225\ [23], \qquad m_b(m_b) = 4.2\ [23],$$
$$m_c(m_b) = 1.3 \pm 0.2\ [23],$$
$$m_u(2\ \mathrm{GeV}) = 2.15 \pm 0.15\ (\mathrm{MeV})\ [41],$$
$$m_d(2\ \mathrm{GeV}) = 4.70 \pm 0.20\ (\mathrm{MeV})\ [41],$$
$$m_s(2\ \mathrm{GeV}) = 93.8 \pm 1.3 \pm 1.9\ (\mathrm{MeV})\ [41], \quad (14)$$

where the superscript (5) in the parameter $\Lambda_{\bar{MS}}$ corresponds to number of active flavor.

(ii) CKM parameters and B_s meson lifetime

$$V_{ub} = 0.00365 \pm 0.00012\ [11],$$
$$\gamma = (73.5^{+4.2}_{-5.1})^\circ\ [11]$$
$$V_{cb} = 0.04214 \pm 0.00076\ [11],$$
$$\tau_{B_s} = (1.509 \pm 0.004) \times 10^{-12}\ \mathrm{s}\ [11]. \quad (15)$$

(iii) Gegenbauer moments

$$\alpha_1^K = 0.06 \pm 0.03\ [1],$$
$$\alpha_2^K = 0.25 \pm 0.15\ [1],$$
$$\lambda_{B_s} = 300 \pm 100\ (\mathrm{MeV})\ [1]. \quad (16)$$

(iv) Form factor (at $q^2 = 0$) and decay constants

$$F_0^{B_s\to K} = 0.323 \pm 0.063\ [42],$$
$$f_{B_s} = 0.228 \pm 0.010\ [43],$$
$$f_K = 0.156 \pm 0.007\ [44]. \quad (17)$$

(v) Annihilation and hard spectator parameters

$$\rho_A = 1 \pm 0.1\ [1], \qquad \phi_A = (-55 \pm 20)^\circ\ [1],$$
$$X_H = 2.4 \pm 0.024\ [23]. \quad (18)$$

By using the above input parameters, we get the predicted values of the prominent observables as

$$\mathcal{BR} = (38.22^{+1.41+9.58+1.193+2.884}_{-1.41-9.58-1.193-2.884}) \times 10^{-6},$$
$$\mathcal{C}_{KK} = (-10.87^{+0.34+1.10++0.20+0.37}_{-0.34-1.10-0.20-0.37}) \times 10^{-2},$$
$$\mathcal{S}_{KK} = (26.09^{+0.817+2.50+0.36+0.8}_{-0.817-2.50-0.36-0.8}) \times 10^{-2}. \quad (19)$$

The sequence of the parameters to the uncertainties of the above observables (19) include as follows:

(i) First: CKM parameters-$|V_{cb}|$, $|V_{ub}|$, and γ,

(ii) Second: quark masses, form factor, and decay constants,

(iii) Third: Gegenbauer moments in the expansion of distribution amplitude,
(iv) Fourth: power corrections to hard spectator and annihilation contribution.

III. Z' MODEL

In this section, we discuss the effects of new physics associated with Z' model on the observables of $B_s \to K^+K^-$ decay process. We constrain the Z' new couplings by using the experimental limits on $B_s \to \ell\ell$ (where ℓ is any charged leptons), mediated by the FCNC transitions $b \to s\ell\ell$. These are the theoretically cleanest B decays as the only nonperturbative quantity involved in the description of these processes is the B_s meson decay constant.

A. $B_s \to \ell^+\ell^-$ ($\ell = e, \mu, \tau$) processes

In the SM, the effective Hamiltonian for quark level transitions $b \to s\ell^+\ell^-$ is given by [27,28]

$$\mathcal{H}_{\rm eff} = -\frac{G_F}{\sqrt{2}}[\lambda_t^{(q)}\mathcal{H}_{\rm eff}^{(t)} + \lambda_u^{(q)}\mathcal{H}_{\rm eff}^{(u)}] + \text{H.c.}, \qquad (20)$$

where

$$\mathcal{H}_{\rm eff}^{(u)} = C_1(\mathcal{O}_1^c - \mathcal{O}_1^u) + C_2(\mathcal{O}_2^c - \mathcal{O}_2^u),$$
$$\mathcal{H}_{\rm eff}^{(t)} = C_1\mathcal{O}_1^c + C_2\mathcal{O}_1^u) + \sum_{i=3}^{10} C_i\mathcal{O}_i. \qquad (21)$$

Here $\lambda_k^{(q=s)} = V_{kb}V_{kq=s}^*(k = u, c, t)$ is the CKM parameter and C_i's ($i = 1, \ldots, 10$) are the Wilson coefficients. Using effective Hamiltonian (20), the transition amplitude for this process is given as

$$\mathcal{M}(B_s \to \ell^+\ell^-) = i\frac{G_F\alpha}{\sqrt{2}\pi}V_{tb}V_{ts}^* f_{B_s}C_{10}m_\ell(\bar{\ell}\gamma_5\ell), \qquad (22)$$

where α is the fine structure constant. Here, we have used the vacuum insertion method to define the decay constant in the matrix element as

$$\langle 0|\bar{s}\gamma^\mu\gamma_5 b|B_s^0\rangle = if_{B_s}p_B^\mu, \qquad (23)$$

where $p_B^\mu = p_{\ell^+}^\mu + p_{\ell^-}^\mu$. In general, from Eq. (22), the associated branching ratio is given as [29]

$$\mathcal{BR}(B_s \to \ell^+\ell^-) = \frac{G_F^2\tau_{B_s}}{16\pi^3}\alpha^2 f_{B_s}^2 m_{B_s} m_\ell^2 |V_{tb}V_{ts}^*|^2|C_{10}|^2 \times\sqrt{1 - \frac{4m_\ell^2}{m_{B_s}^2}}. \qquad (24)$$

Using the B_s decay constant from [43] and remaining input parameters from PDG [11], the branching ratio predictions are presented below. The errors in the SM results are coming mainly from decay constant and CKM matrix elements. Here we also show the corresponding experimental limits for all leptonic decay modes [11].

$$\mathcal{BR}^{\rm SM}_{B_s\to\mu^+\mu^-} = (3.56 \pm 0.33) \times 10^{-9}, \qquad \mathcal{BR}^{\rm Exp}_{B_s\to\mu^+\mu^-} = (2.7^{+0.6}_{-0.5}) \times 10^{-9},$$
$$\mathcal{BR}^{\rm SM}_{B_s\to\tau^+\tau^-} = (7.64 \pm 0.72) \times 10^{-7}, \qquad \mathcal{BR}^{\rm Exp}_{B_s\to\tau^+\tau^-} < 6.8 \times 10^{-3},$$
$$\mathcal{BR}^{\rm SM}_{B_s\to e^+e^-} = (8.40 \pm 0.79) \times 10^{-14}, \qquad \mathcal{BR}^{\rm Exp}_{B_s\to e^+e^-} < 2.8 \times 10^{-7}. \qquad (25)$$

Though $B_s \to \ell^+\ell^-$ decays occur only at one-loop level in the SM, these processes can occur at tree level in the presence of new Z' gauge boson arising due to the $U(1)'$ gauge extension of the SM. The effective Hamiltonian corresponding to the transition $b \to s\ell^+\ell^-$ process is given by [31,32]

$$\mathcal{H}_{\rm eff}^{Z'} = -\frac{2G_F}{\sqrt{2}}V_{tb}V_{ts}^*\left(\frac{g'M_Z}{g_1M_{Z'}}\right)^2\left[\frac{U_{bs}^LU_{\ell\ell}^L}{V_{tb}V_{ts}^*}(\bar{s}b)_{V-A}(\bar{\ell}\ell)_{V-A}\right. \left. - \frac{U_{bs}^LU_{\ell\ell}^R}{V_{tb}V_{ts}^*}(\bar{s}b)_{V-A}(\bar{\ell}\ell)_{V+A}\right] + \text{H.c.}, \qquad (26)$$

where $g_1(g')$ is the coupling constant of $Z(Z')$ boson. According to the SM effective Hamiltonian (20), the Hamiltonian in Z' can be written as

$$\mathcal{H}_{\rm eff}^{Z'} = -\frac{G_F}{\sqrt{2}}V_{tb}V_{ts}^*[C_9^{Z'}O_9 + C_{10}^{Z'}O_{10}] + \text{H.c.}, \qquad (27)$$

where the new Wilson coefficients are given as

$$C_9^{Z'} = -2\left(\frac{g' M_Z}{g_1 M_{Z'}}\right)^2 \frac{U_{bs}^L}{V_{tb}V_{ts}^*}(U_{\ell\ell}^L + U_{\ell\ell}^R) = -2\left(\frac{g' M_Z}{g_1 M_{Z'}}\right)^2 \frac{|U_{bs}^L|e^{i\phi_s}}{V_{tb}V_{ts}^*}(U_{\ell\ell}^L + U_{\ell\ell}^R),$$
$$C_{10}^{Z'} = 2\left(\frac{g' M_Z}{g_1 M_{Z'}}\right)^2 \frac{U_{bs}^L}{V_{tb}V_{ts}^*}(U_{\ell\ell}^L - U_{\ell\ell}^R) = 2\left(\frac{g' M_Z}{g_1 M_{Z'}}\right)^2 \frac{|U_{bs}^L|e^{i\phi_s}}{V_{tb}V_{ts}^*}(U_{\ell\ell}^L - U_{\ell\ell}^R), \quad (28)$$

with ϕ_s is the associated weak phase of U_{bs}. We consider $\frac{g'}{g_1} \sim 1$ with the assumption that both the $U(1)$ groups have same origin from some grand unified theory. For a TeV-scale Z' boson, their ratio of masses $M_Z/M_{Z'}$ will be $\sim 10^{-1}$. In this analysis, the coupling of Z' boson to leptons $U_{\ell\ell}^{L(R)}$ are considered to be SM-like. Now, comparing the theoretical values of $B_s \to \ell\ell$ branching ratios with their corresponding 1σ range of experimental data, we constrain the new $Z' - b - s$ coupling (U_{bs}) and weak phase (ϕ_s) as shown in Fig. 1. From this figure, the allowed range of U_{bs} and ϕ_s parameters of Z' model is given as

$$0.675 \lesssim |U_{bs}| \lesssim 0.99,$$
$$\text{for } 0° \le \phi_s \le \frac{5\pi}{18} \text{ and } \frac{7\pi}{4} \le \phi_s \le 2\pi. \quad (29)$$

B. Impact on nonleptonic $B_s \to KK$ decay mode

Now, we will discuss the impact of family nonuniversal Z' gauge boson on the $B_s \to K^+K^-$ decay mode. The effective Hamiltonian describing the $b \to sq\bar{q}$ ($q = u, d$) transition for $B_s \to K^+K^-$ decay mode is given as [16]

$$\mathcal{H}_{\rm eff}^{Z'} = \frac{2G_F}{\sqrt{2}}\left(\frac{g' M_Z}{g_1 M_{Z'}}\right)^2 U_{bs}^L (\bar{s}b)_{V-A} \times \sum_q [U_{qq}^L (\bar{q}q)_{V-A} + U_{qq}^R (\bar{q}q)_{V+A}] + \text{H.c.} \quad (30)$$

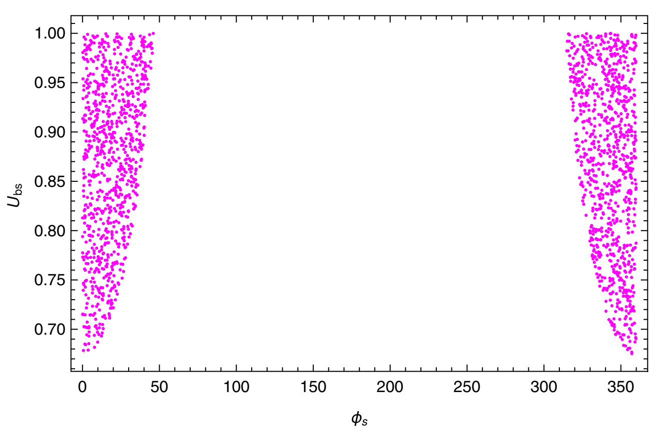

FIG. 1. The allowed region in the new coupling parameter space obtained from the branching ratios of leptonic $B_s \to \ell^+\ell^-(\ell = e, \mu, \tau)$ processes in Z' model.

Due to hermiticity of effective Hamiltonian, the diagonal elements of $U_{qq}^{L(R)}$ are real where the nondiagonal elements of $U_{bs}^{L(R)}$ might be complex along with a phase ϕ_s. Now, comparing the effective Hamiltonian of Z' model of Eq. (30) with the general effective Hamiltonian

$$\mathcal{H}_{\rm eff} = -\frac{G_F}{\sqrt{2}} V_{tb}V_{ts}^* \sum_q [C_9' O_9 + C_7' O_7], \quad (31)$$

we obtain

$$C'_{9(7)} = -\frac{4}{3}\left(\frac{g' M_Z}{g_1 M_{Z'}}\right)^2 U_{bs}^L (U_{uu}^{L(R)} - U_{dd}^{L(R)}), \quad (32)$$

where C_9', C_7' are the new Wilson coefficients arising due to Z' gauge boson. Many studies have been done in [16,33–37] with the manifestation of electroweak contribution assuming $U_{uu}^{L(R)} \simeq -2U_{dd}^{L(R)}$. Thus,

$$C'_{9(7)} = 4\left(\frac{g' M_Z}{g_1 M_{Z'}}\right)^2 \frac{U_{bs}^L U_{dd}^{L(R)}}{V_{tb}V_{ts}^*}. \quad (33)$$

Now, for convenience, these coefficients can be written in the following parametric form as

$$C'_{9(7)} = 4\left(\frac{g' M_Z}{g_1 M_{Z'}}\right)^2 U_{bs}^L = 4\left(\frac{g' M_Z}{g_1 M_{Z'}}\right)^2 \frac{|U_{bs}^L|e^{i\phi_s}}{V_{tb}V_{ts}^*}, \quad (34)$$

where the assumption of $U_{qq}^{L(R)} \sim 1$ has been taken out from experimental data of B_s meson [15]. The decay amplitude in the presence of additional Z' boson can be written as

$$\mathcal{A}_{B_s^0 \to K^+K^-} = A_{K\bar{K}}\Big[\delta_{pu}\alpha_1 + \alpha_4^p + \alpha_{4,EW}^p + \beta_3^p + \beta_4^p - \frac{1}{2}\beta_{3,EW}^p - \frac{1}{2}\beta_{4,EW}^p\Big] + B_{\bar{K}K}[\delta_{pu}b_1 + b_4^p + b_{4,EW}^p] - \zeta_t\Big[A_{K\bar{K}}\Big(\tilde{\alpha}_4^p + \tilde{\alpha}_{4,EW}^p + \tilde{\beta}_3^p - \frac{1}{2}\tilde{\beta}_{3,EW}^p\Big)\Big], \quad (35)$$

where terms $\tilde{\alpha}$ and $\tilde{\beta}$ arise due to new physics contributions. We can represent the above transition amplitude in the parametrized form as

$$\mathcal{A} = A^{SM} - \zeta_t A^{NP} = \zeta_c A_c[1 + \wp a e^{i(\delta_1-\gamma)} - \wp' b e^{(\delta_2+\phi_s)}]. \tag{36}$$

In addition to $\wp$ and a, given in the previous section, the new parameters in the above amplitude are defined as $b = |\frac{\zeta_t}{\zeta_c}|$, $\wp' = |\frac{\mathcal{A}_{NP}}{\mathcal{A}_c}|$. δ_2 is the relative strong phase and is given by $\delta_2 = \mathrm{Arg}(\frac{\mathcal{A}_{NP}}{\mathcal{A}_c})$.

The CP-averaged branching ratio can be written as

$$\mathcal{BR} = \frac{\tau_{B_s} p_c}{8\pi m_{B_s}^2}|\zeta_c A_c|^2[\mathcal{G} + 2\wp a \cos\delta_1 \cos\gamma - 2\wp' b \cos\delta_2 \cos\phi_s - 2\wp\wp' ab \cos(\delta_1-\delta_2)\cos(\gamma+\phi_s)]. \tag{37}$$

The direct CP asymmetry is given as

$$\mathcal{C}_{KK} = -\frac{2[ra\sin\delta_1\sin\gamma + \wp' b\sin\delta_2\sin\phi_s + \wp\wp' ab\sin(\delta_2-\delta_1)\sin(\gamma+\phi_s)]}{[\mathcal{G} + 2(\wp a\cos\delta_1\cos\gamma - 2\wp' b\cos\phi_s\delta_2 - 2\wp\wp' bb'\cos(\gamma+\phi_s)\cos(\delta_2-\delta_1))]}. \tag{38}$$

The mixing-induced CP asymmetry can be represented as

$$\mathcal{S}_{KK} = \frac{\mathcal{M}}{\mathcal{G} + 2\wp a\cos\delta_1\cos\gamma - 2\wp' b\cos\delta_2\cos\phi_s - 2\wp\wp' ab\cos(\delta_1-\delta_2)\cos(\gamma+\phi_s)}, \tag{39}$$

where $\mathcal{G} = 1 + (\wp a)^2 + (\wp' b)^2$ and

$$\mathcal{M} = \sin 2\beta + 2\wp a\cos\delta_1\sin(2\beta+\gamma) - 2\wp' b\cos\delta_2\sin(2\beta-\phi_s) + (\wp a)^2\sin(2\beta+2\gamma) \tag{40}$$

$$+(\wp' b)^2\sin(2\beta-2\phi_s) - 2\wp\wp' ab\cos(\delta_1-\delta_2)\sin(2\beta+\gamma-\phi_s). \tag{41}$$

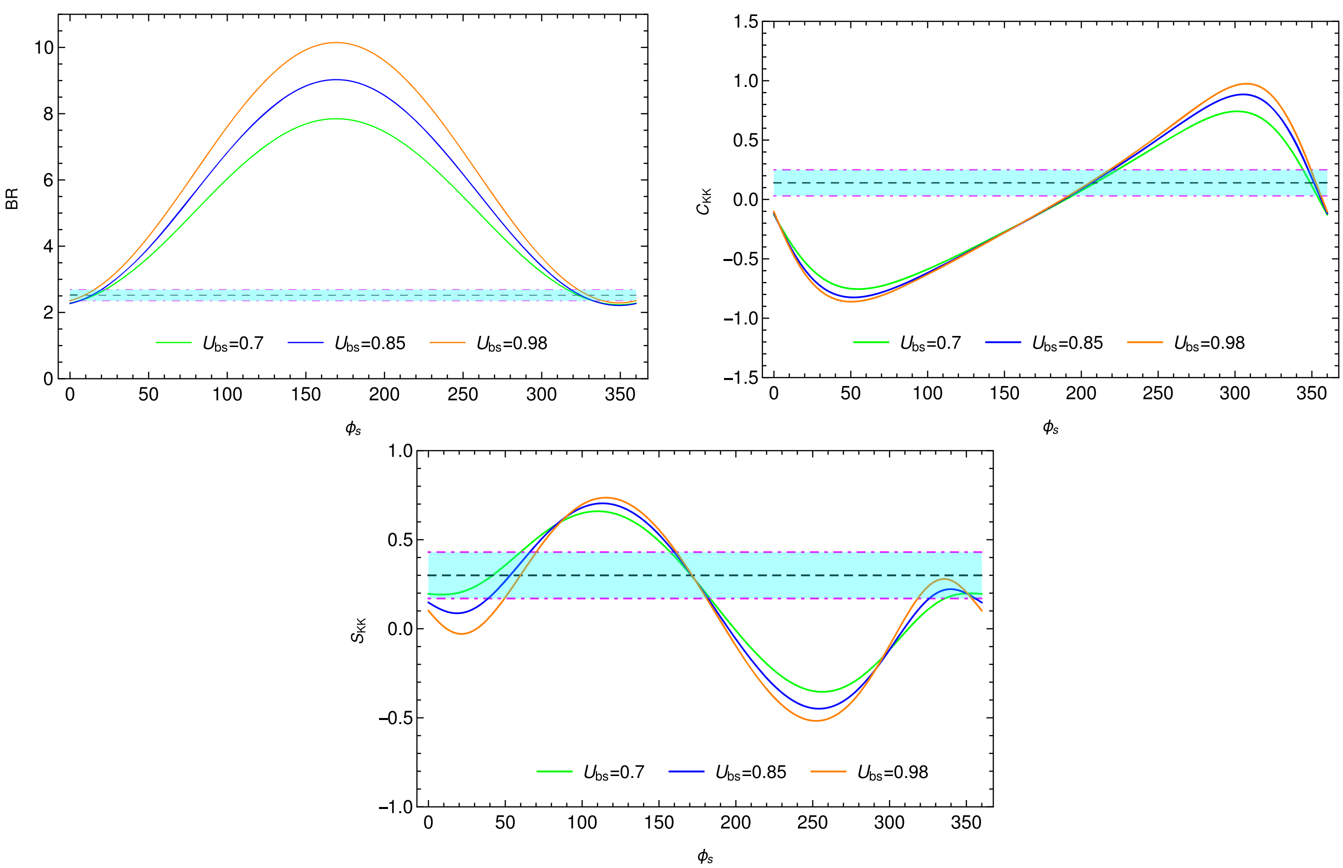

FIG. 2. Variation of CP-averaged branching ratio (in the units of 10^{-5}) (top-left panel), direct CP asymmetry (top-right panel), and mixing-induced CP asymmetry (bottom panel) (in %) with the new weak phase ϕ_s for different $|U_{bs}|$ entries. The black color horizontal dotted line represents the central experimental value, whereas the magenta dotted lines along with cyan colored region denote its 1σ error limit.

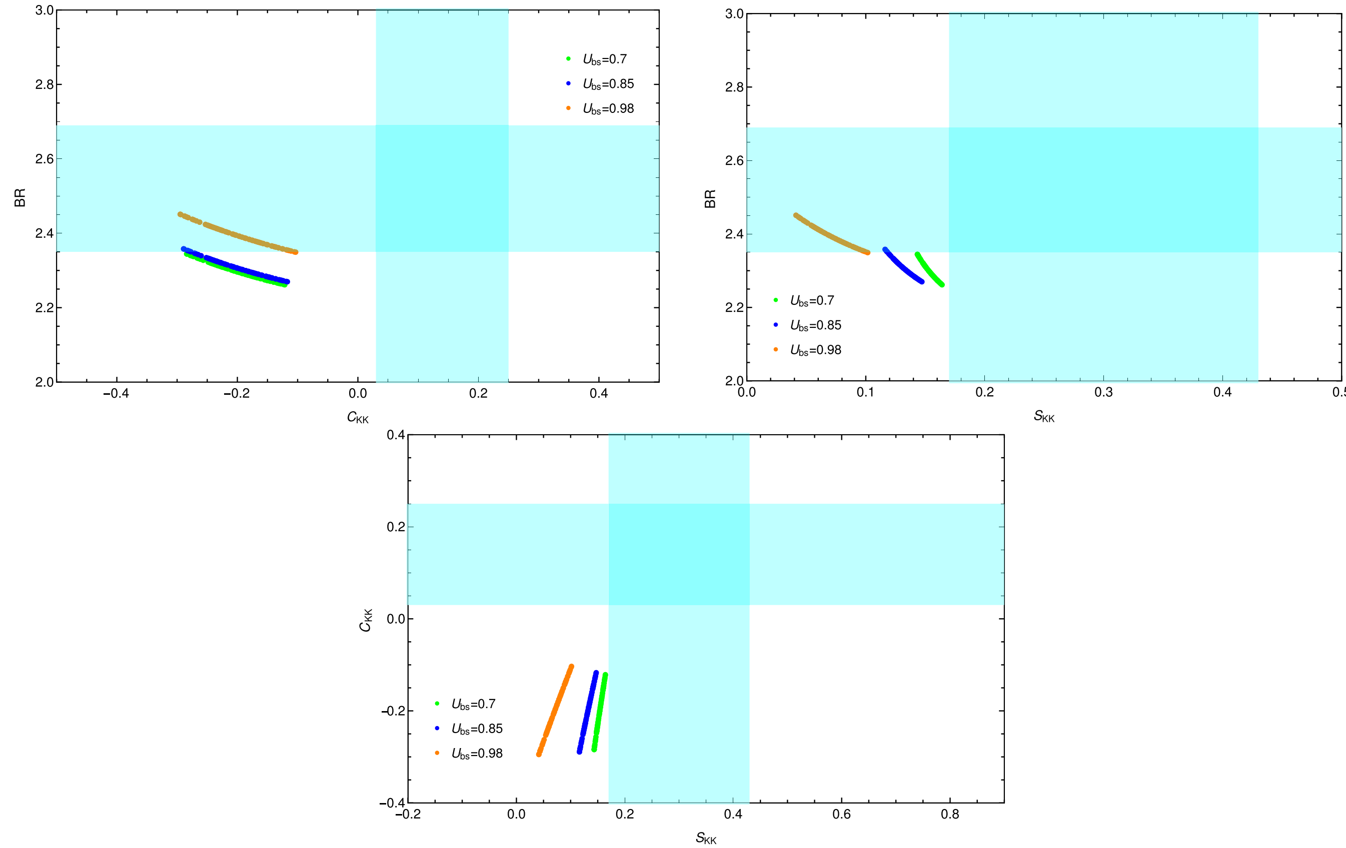

FIG. 3. Correlation plots of CP-averaged branching ratio (in the units of 10^{-5}) with direct CP asymmetry (top-left panel) and mixing-induced CP asymmetry (top-right panel) (in %), and direct CP asymmetry with mixing induced CP asymmetry (bottom panel). The shaded cyan colored region signifies 1σ range of experimental data in each plot.

After collecting the detailed expression for CP-averaged branching ratio and the CP-violating parameters in the presence of new Z' gauge boson, we now proceed for numerical analysis for these observables. Using the allowed parameter space from Eq. (29), we display the variation of CP-averaged branching ratio (top-left panel), direct CP violation (top-right panel), and mixing-induced CP asymmetry (bottom panel) with respect to mixing weak phase ϕ_s with some benchmark entries of U_{bs}(color) as 0.7 (green), 0.85 (blue), and 0.98 (orange) in Fig. 2. As we notice from the top-left one, for all entries of U_{bs} values along with the value of ϕ_s below 20° and after 320°, the NP effects on branching ratios do contribute within 1σ range of experimental data. On the other side, if we observe the CP-violating parameters in the new physics scenario, both C_{KK} and S_{KK} are accommodating within 1σ limit. Figure 3 depicts the correlations among all the discussed observables. In this figure, the top-left (right) panel displays $\mathrm{BR} - C_{KK}(S_{KK})$ correlations and the plot in the bottom panel shows a relationship between C_{KK} and S_{KK}. If we observe carefully to the correlation plots for both top-left and top-right panels, with the benchmark value of $U_{bs} = 0.98$, the observables accommodate the experimental data completely within 1σ error limit whereas in the bottom panel,

TABLE III. Predicted values of CP-averaged branching ratio and CP-violating observables for different benchmark values of $U_{bs}(Q_{bs})$ and ϕ_s parameters in the Z' (VLDQ) model.

Model	$U_{bs}(Q_{bs})$	ϕ_s	$\mathcal{BR}$	C_{KK}	S_{KK}
Z' model	0.85	0°	22.69×10^{-6}	−0.10	0.14
		50°	39.5×10^{-6}	−0.82	0.26
		315°	28.03×10^{-6}	0.86	0.06
	0.9	0°	22.90×10^{-6}	−0.11	0.12
		50°	40.69×10^{-6}	−0.84	0.23
		315°	28.55×10^{-6}	0.89	0.08
	0.98	0°	23.55×10^{-6}	−0.10	0.10
		50°	42.93×10^{-5}	−0.86	0.17
		315°	29.71×10^{-6}	0.95	0.12
VLDQ model	2×10^{-4}	0°	21.23×10^{-6}	−0.21	0.33
		75°	38.28×10^{-6}	−0.20	0.69
		285°	33.27×10^{-6}	−0.02	−0.25
	5×10^{-4}	0°	5.63×10^{-6}	−0.79	0.50
		75°	48.26×10^{-6}	−0.25	0.96
		285°	35.73×10^{-6}	0.13	−0.87
	8×10^{-4}	0°	3.02×10^{-6}	−2.91	−0.59
		75°	70.40×10^{-6}	−0.26	0.86
		285°	50.34×10^{-6}	0.18	−0.96

no observables are accommodating within 1σ. We have shown the predicted results of branching ratios, CP-violating observables for different values of U_{bs} and ϕ_s in the top section of Table III.

IV. VECTORLIKE DOWN QUARK (VLDQ) MODEL

Here we study the minimal extension of SM where the quark sector is expanded by an extra vectorlike down quark. Because of this, we obtain a 4×4 matrix $V_{i\alpha}$ ($i=u,c,t,t'$ and $\alpha=d,s,b,b'$) from which the interaction of this extra down-type quark with the SM quarks could be obtainable and scrutinize the deviations of the unitarity relation of the CKM matrix. This mixing provides a remarkable study of flavor changing neutral current (FCNC) interaction where Z particle is mediated through tree level contribution. In general, this model includes the following Lagrangian [21]:

$$\mathcal{L}_Z = \frac{g}{2\cos\theta_W}[\bar{u}_{Li}\gamma^\mu u_{Li} - \bar{d}_{L\alpha}Q_{\alpha\beta}\gamma^\mu d_{L\alpha} - 2\sin^2\theta_W J^\mu_{em}]Z_\mu,$$

where L denotes the left-handed chiral particles, i and α,β denote the generation indices for up-type and down-type quarks, respectively. The second term in the above Lagrangian corresponds to the mixing in the down-type quark sector and the matrix $Q_{\alpha\beta}$ can be represented as

$$Q_{\alpha\beta} = \sum_{i=u,c,t} V^\dagger_{\alpha i}V_{i\beta} = \delta_{\alpha\beta} - V^*_{4\alpha}V_{4\beta}. \tag{42}$$

Here V is not unitary as an extra down-type vector like quark of charge $(-\frac{1}{3})$ has been added to the SM. It provides a new signal to probe the physics beyond the SM and modify the CP asymmetries and branching ratio predictions. We constrain the new parameters from the $\mathrm{Br}(B_s\to\ell^+\ell^-)$ to be presented in the subsequent section.

A. $B_s\to\ell^+\ell^-$ ($\ell=e,\mu,\tau$) processes

Though $B_s\to\ell^+\ell^-$ process are suppressed in the SM, but can be significant in the presence of extra vectorlike down quark particle where Z is mediated at tree level whose contribution provides the physics beyond the SM. The branching ratio of $B_s\to\ell^+\ell^-$ in Z mediated VLDQ model is given by [38]

$$\mathcal{BR}(B_s\to\ell^+\ell^-) = \frac{G_F^2\alpha^2 m_{B_s} m_\ell^2 f_{B_s}^2\tau_{B_s}}{16\pi^3}|V_{tb}V^*_{ts}|^2 \times\sqrt{1-4\left(\frac{m_\ell^2}{m_{B_s}^2}\right)}|C_{10}^{\rm tot}|^2, \tag{43}$$

where

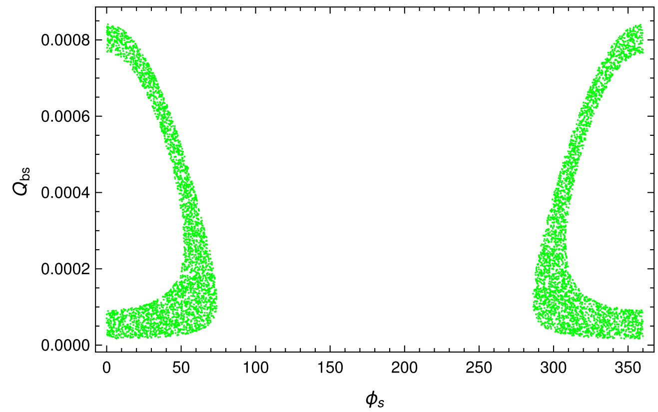

FIG. 4. The allowed region in the new coupling parameter space obtained from all the branching ratios of leptonic $B_s\to\ell^+\ell^-$ ($\ell=e,\mu,\tau$) processes in VLDQ model.

$$C_{10}^{\rm tot} = C_{10} - \frac{\pi}{\alpha}\frac{Q_{bs}}{V_{tb}V^*_{ts}}. \tag{44}$$

Here the second term provides the NP contribution to the decay amplitude where the parameter Q_{bs} defines the coupling of b to s quark at tree level. Using the theoretical and experimental values of $B_s\to\ell\ell$ (25)), the constraint on $Q_{bs}-\phi_s$ parameters is presented in Fig 4. The ranges obtained from the constrained plots are given as

$$1.69\times10^{-5}\lesssim|Q_{bs}|\lesssim 8.4\times10^{-4}, \quad \text{for } 0^\circ\le\phi_s\le\frac{5\pi}{12} \text{ and } \frac{19\pi}{12}\le\phi_s\le 2\pi. \tag{45}$$

B. Impact on $B_s\to KK$ mode

The effective Hamiltonian corresponding to new interaction describing $b\to sq\bar{q}$ can be represented as

$$\mathcal{H}^Z_{\rm eff} = -\frac{G_F}{\sqrt{2}}V_{tb}V^*_{ts}[\tilde{C}_3O_3+\tilde{C}_7O_7+\tilde{C}_9O_9],$$

where the new Wilson coefficients at the M_Z scale are given as [20,39]

$$\tilde{C}_3(M_Z) = \frac{1}{6}\frac{Q_{bs}}{V_{tb}V^*_{ts}}, \quad \tilde{C}_7(M_Z) = \frac{2}{3}\frac{Q_{bs}}{V_{tb}V^*_{ts}}\sin^2\theta_W, \quad \tilde{C}_9(M_Z) = -\frac{2}{3}\frac{Q_{bs}}{V_{tb}V^*_{ts}}(1-\sin^2\theta_W). \tag{46}$$

Here $Q_{bs}=|Q_{bs}|e^{i\phi_s}$ and $\sin^2\theta_W=0.231$. As the new couplings are in M_Z scale, so these can be evolved to m_b scale employing renormalization group equation [22]. By using RGE, these three couplings can be generated and we consider the above values from Ref. [40].

Now, using the unitarity condition from Eq. (42), we get

$$\xi_u + \xi_c + \xi_t = Q_{bs}. \quad (47)$$

To this relation, we can express the decay amplitude along with the new physics contributions as

$$\begin{aligned}\mathcal{A}_{B_s^0\to K^+K^-} = A_{K\bar{K}}\bigg[&\delta_{pu}\alpha_1 + \alpha_4^p + \alpha_{4,EW}^p + \beta_3^p + \beta_4^p \\ &-\frac{1}{2}\beta_{3,EW}^p - \frac{1}{2}\beta_{4,EW}^p\bigg] \\ &+ B_{\bar{K}K}[\delta_{pu}b_1 + b_4^p + b_{4,EW}^p] \\ &- Q_{bs}\left[A_{K\bar{K}}\left(\tilde{\alpha}_4^p + \tilde{\alpha}_{4,EW}^p + \tilde{\beta}_3^p - \frac{1}{2}\tilde{\beta}_{3,EW}^p\right)\right]. \end{aligned} \quad (48)$$

Here, $\tilde{\alpha}^p$ and $\tilde{\beta}^p$ provide the dominant contributions to NP amplitude which contains all the new couplings as given in Eq. (43). Symbolically, the full amplitude can be written as

$$\begin{aligned}\mathcal{A} &= \xi_u\mathcal{A}_u + \xi_c\mathcal{A}_c - Q_{bs}\mathcal{A}_{NP} \\ &= \xi_c A_c[1 + \varrho a' e^{i(\delta_1'-\gamma)} - \varrho' b' e^{i(\delta_2'+\phi_s)}], \end{aligned} \quad (49)$$

where

$$a' = \left|\frac{\xi_u}{\xi_c}\right|, \quad b' = \left|\frac{Q_{bs}}{\xi_c}\right|, \quad \varrho = \left|\frac{A_u}{A_c}\right|, \quad \varrho' = \left|\frac{A_{NP}}{A_c}\right|. \quad (50)$$

Here, γ is the weak phase of V_{ub}, ϕ_s is the weak phase of Q_{bs}, and $\delta_1'(\delta_2')$ is the relative strong phase between A_u and $A_c(A_{NP}$ and $A_c)$. From the parametrized amplitude, the CP-averaged branching ratio can be written as

$$\begin{aligned}\mathcal{BR} = \frac{\tau_{B_s} p_c}{8\pi m_{B_s}^2}|\xi_c A_c|^2[&\mathcal{G}' + 2\varrho a' \cos\delta_1' \cos\gamma \\ &- 2\varrho' b' \cos\delta_2' \cos\phi_s \\ &- 2\varrho\varrho' a' b' \cos(\delta_1 - \delta_2')\cos(\gamma + \phi_s)]. \end{aligned} \quad (51)$$

On the other hand, the direct CP asymmetry can be written as

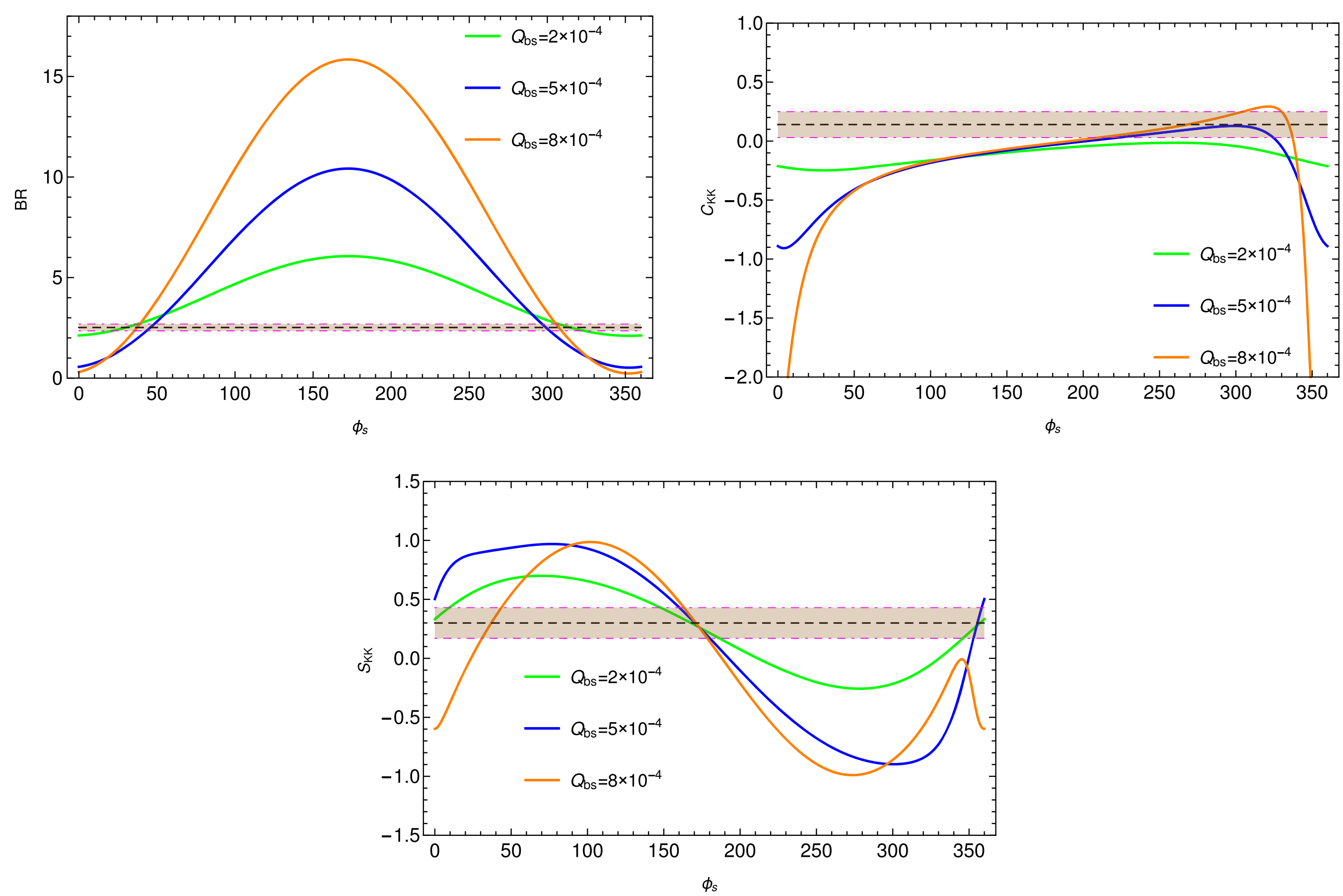

FIG. 5. Variation of CP-averaged branching ratio (in the units of 10^{-5}) (top-left panel), direct CP asymmetry (top-right panel), and mixing-induced CP asymmetry (bottom panel) with the new weak phase ϕ_s for different $|U_{bs}|$ entries. The horizontal line (dotted black color) represents the central experimental value, whereas the dot-dashed lines (magenta color) along with brown colored shaded region denote the 1σ error limit of experimental values.

$$\mathcal{C}_{KK} = -\frac{2[\varrho a' \sin\delta_1' \sin\gamma + \varrho' b' \sin\delta_2' \sin\phi_s + \varrho\varrho' a' b' \sin(\delta_2' - \delta_1)\sin(\gamma + \phi_s)]}{[\mathcal{G}' + 2(\varrho a' \cos\delta_1' \cos\gamma - 2\varrho' b' \cos\phi_s \delta_2' - 2\varrho\varrho' a' b' \cos(\gamma + \phi_s)\cos(\delta_2' - \delta_1'))]}. \tag{52}$$

One can obtain the mixing-induced CP asymmetry parameter as

$$\mathcal{S}_{KK} = \frac{\mathcal{M}'}{\mathcal{G}' + 2\varrho a' \cos\delta_1' \cos\gamma - 2\varrho_2 b' \cos\delta_2' \cos\phi_s - 2\varrho_1\varrho_2 a' b' \cos(\delta_1' - \delta_2')\cos(\gamma + \phi_s)}, \tag{53}$$

where $\mathcal{G}' = 1 + (\varrho a')^2 + (\varrho' b')^2$ and

$$\mathcal{M} = \sin 2\beta_s + 2ra' \cos\delta_1 \sin(2\beta_s + \gamma) - 2r' b' \cos\delta_2 \sin(2\beta_s - \phi_s) + (ra')^2 \sin(2\beta_s + 2\gamma) \tag{54}$$

$$+ (r' b')^2 \sin(2\beta_s - 2\phi_s) - 2rr' a' b' \cos(\delta_1 - \delta_2)\sin(2\beta_s + \gamma - \phi_s). \tag{55}$$

In Fig. 5, we present the variation of CP-averaged branching ratios (top-left panel), direct (top-right panel), and mixing induced (bottom panel) CP asymmetries with respect to the weak phase ϕ_s for three benchmark Q_{bs} values. Here the colors green, blue, and orange solid lines represent the predictions obtained by using $Q_{bs} = 2 \times 10^{-4}$, 5×10^{-4}, and 8×10^{-4}, respectively. For the entries of ϕ_s below 50° and above 290°, and with all the discussed benchmark points of Q_{bs}, the predicted branching of $B_s \to KK$ is accommodating within 1σ range of experimental central value. We also notice that the CP-violating parameters are also explained within 1σ data, but in C_{KK} the value $Q_{bs} = 2 \times 10^{-4}$ could not accommodate. The correlation plots among all the observables are shown in Fig. 6 for the

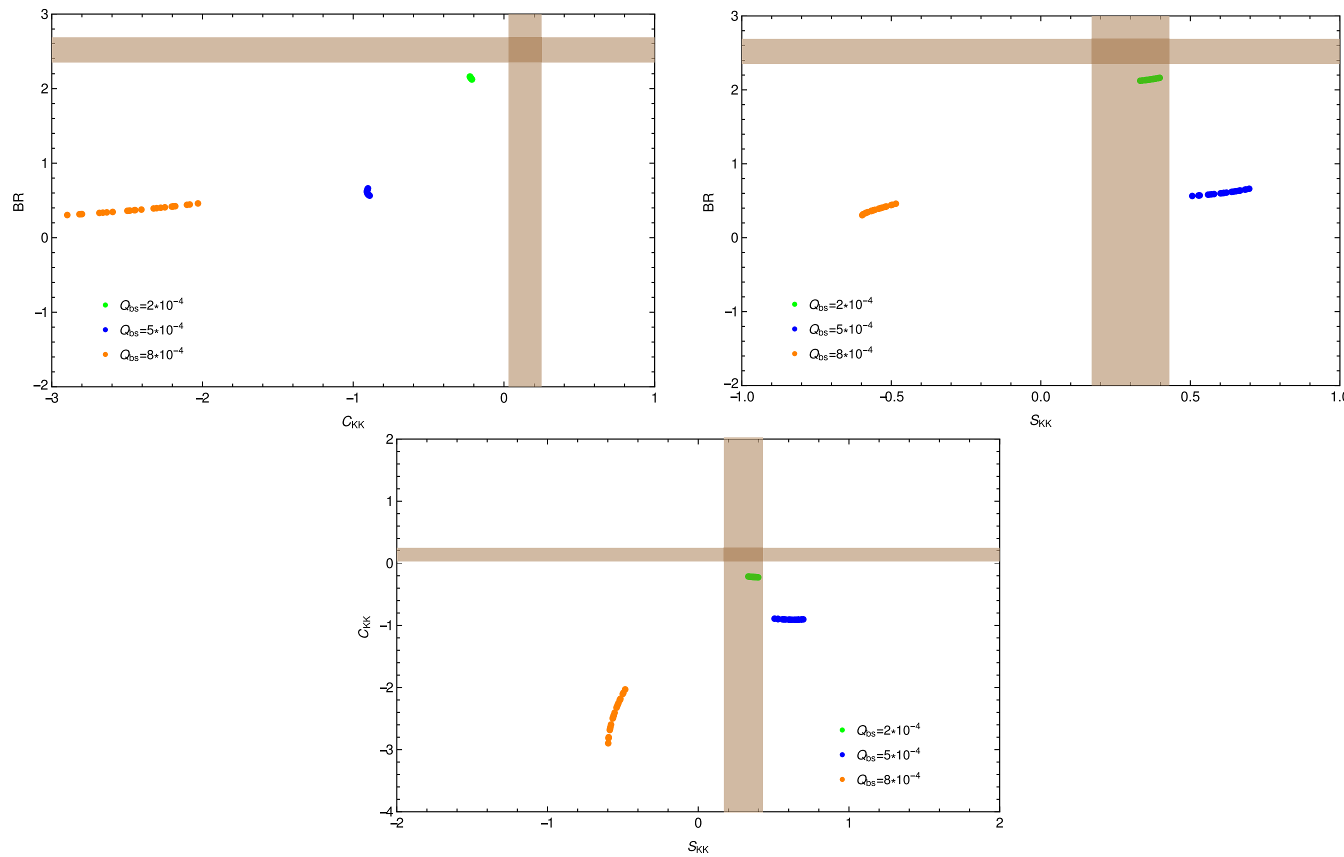

FIG. 6. Correlation plots of CP-averaged branching ratio (in the units of 10^{-5}) with direct CP asymmetry (top-left panel) and mixing-induced CP asymmetry (top-right panel) (in %), and direct CP asymmetry with mixing-induced CP asymmetry (bottom panel). The brown shaded region addresses 1σ range of experimental value.

same inputs of Q_{bs}. With the careful observation, we bring to the notice in the top-left panel that for all entries of Q_{bs}, it does not accommodate the experimental data within 1σ limit. In the top-right and bottom panel, with the value of $Q_{bs} = 2\times10^{-4}$, the observables lie within 1σ limit whereas for $Q_{bs} = 5\times10^{-4}$ and 8×10^{-4} values the correlations among the observables could not accommodate within 1σ. The predicted results of branching ratio, CP-violating observables for different values of Q_{bs} and ϕ_s are shown in the bottom section of Table III.

V. CONCLUSION

To conclude, we have investigated the prominent observables of $B_s \to K^+K^-$, a penguin-dominated decay mode occurring at quark level transition $b\to s$, both in standard model and beyond the SM scenarios. In the new physics scenario, we consider both the Z' and vectorlike down quark model, where the consequence of the former one is nothing but the minimal extension of SM having $U(1)'$ gauge group added to it and the later one provides the interaction of Z mediated FCNC at the tree level. We have constrained the NP parameter associated with "$Z^{(\prime)}-b-s$" interactions from the branching ratios of all leptonic B_s decay modes and mainly checked whether the new physics coupling has impact on the physical observables of nonleptonic $B_s \to K^+K^-$ decay mode. We have found that the CP-averaged branching ratio could accommodate the experimental data within 1σ range in Z' model. On the other hand, it has deviated significantly from the SM results for sizable new physics coupling parameters Q_{bs} of VLDQ model. Furthermore, in both models, the CP-violating parameters such as direct and mixing induced have profound deviation in the presence of new physics and accommodate the experimental data.

ACKNOWLEDGMENTS

M. K. M. would like to thank to Department of Science and Technology (DST)- Inspire Fellowship division, Government of India for financial support through ID No. IF160303. M. K. M. would like to acknowledge Professor Anjan Giri for his support and useful discussions.

APPENDIX: DETAILS OF THE PARAMETERS REQUIRED FOR $B_s \to KK$ DECAY

The relevant factorized matrix elements for the decay $B\to M_1M_2$ are given by

$$A_{M_1M_2} = i\frac{G_F}{\sqrt{2}}\begin{cases} m_B^2 F_0^{B\to M_1}(0) f_{M_2}; & \text{for } M_1 = M_2 = P,\\ -2m_V\epsilon^*_{M_1}.p_B A_0^{B\to M_1}(0) f_{M_2}; & \text{for } M_1 = V, M_2 = P,\\ -2m_V\epsilon^*_{M_1}.p_B F_+^{B\to M_1}(0) f_{M_2}; & \text{for } M_1 = P, M_2 = V.\end{cases} \tag{A1}$$

Here the form factor $F_{+,0}$ stand for pseudoscalar meson, A_0 denotes vector meson where as $f_{P(V)}$ signify the decay constant for pseudoscalar (vector) meson. The useful explicit expressions of flavor operators in QCDF (QCD Factorization) read as follows [23]:

$$\begin{aligned}
\alpha_1(M_1M_2) &= a_1(M_1M_2),\\
\alpha_2(M_1M_2) &= a_2(M_1M_2),\\
\alpha_3^p(M_1M_2) &= \begin{cases} a_3(M_1M_2) - a_5(M_1M_2); & \text{for } M_1M_2 = PP, VP,\\ a_3(M_1M_2) + a_5(M_1M_2); & \text{for } M_1M_2 = VV, PV,\end{cases}\\
\alpha_4^p(M_1M_2) &= \begin{cases} a_4^p(M_1M_2) + r_\chi^{M_2} a_6^p(M_1M_2); & \text{for } M_1M_2 = PP, PV,\\ a_4^p(M_1M_2) - r_\chi^{M_2} a_6^p(M_1M_2); & \text{for } M_1M_2 = VV, VP,\end{cases}\\
\alpha_{3,EW}^p(M_1M_2) &= \begin{cases} a_9(M_1M_2) - a_7(M_1M_2); & \text{for } M_1M_2 = PP, VP,\\ a_9(M_1M_2) + a_7(M_1M_2); & \text{for } M_1M_2 = VV, PV,\end{cases}\\
\alpha_{4,EW}^p(M_1M_2) &= \begin{cases} a_{10}^p(M_1M_2) + r_\chi^{M_2} a_8^p(M_1M_2); & \text{for } M_1M_2 = PP, PV,\\ a_{10}^p(M_1M_2) - r_\chi^{M_2} a_8^p(M_1M_2); & \text{for } M_1M_2 = VV, VP,\end{cases}
\end{aligned} \tag{A2}$$

where

$$a_i^p(M_1M_2) = \left(C_i + \frac{C_{i\pm1}}{N_c}\right)N_i(M_2) + \frac{C_{i\pm1}}{N_c}\frac{C_F\alpha_s}{4\pi}\left[V_i(M_2) + \frac{4\pi^2}{N_c}H_i(M_1M_2)\right] + P_i^p(M_2), \tag{A3}$$

with the superscript $p = u, c$. Here the quantity $N_i(M_2)$ also reads as

$$N_i(M_2) = \begin{cases} 0; & i = 6, 8, \\ 1; & \text{otherwise}, \end{cases} \tag{A4}$$

moreover in the above expressions, i runs from 1 to 10. The lower (upper) sign in the expression of flavor operator is validate only when i is even (odd), C_i's are the Wilson coefficients, C_F is the color factor having $N_c = 3$. The contributions such as $V_i(M_2)$ and $H_i(M_1M_2)$ account for vertex corrections, hard spectator interactor interactions which include nonfactorizable short distance corrections, whereas $P_i^p(M_1M_2)$ represents as penguin contractions. The explicit expressions of above corrections are given below.

(i) Vertex corrections [23]

$$V_i(M_2) = \begin{cases} \int_0^1 dx \Phi_{M_2}(x)\left[12\ln\frac{m_b}{\mu} - 18 + g(x)\right], & \text{for } i = 1-4, 9, 10, \\ \int_0^1 dx \Phi_{M_2}(x)\left[-12\ln\frac{m_b}{\mu} + 6 - g(1-x)\right], & \text{for } i = 5, 7, \\ \int_0^1 dx \Phi_{m_2}(x)[-6 + h(x)], & \text{for } i = 6, 8, \end{cases}$$

where

$$\begin{aligned} g(x) &= 3\left(\frac{1-2x}{1-x}\ln x - i\pi\right) \\ &\quad + \left[2Li_2(x) - \ln^2 x + \frac{2\ln x}{1-x} - (3 + 2\pi i)\ln x - (x \leftrightarrow 1-x)\right], \\ h(x) &= 2Li_2(x) - \ln^2 x - (1 + 2\pi i)\ln x - (x \leftrightarrow 1-x). \end{aligned} \tag{A5}$$

The inputs $\Phi_{P,V}(x)$ and $\Phi_{p,v}(x)$ to the above expressions called the leading twist and twist-3 light cone distribution amplitudes are given in [23] depending upon the pseudoscalar ($J^{\mathrm{P}} = 0^-$) or vector meson ($J^{\mathrm{P}} = 1^-$).

(ii) Hard spectator interactions [23]

$$H_i(M_1M_2) = \frac{B_{M_1M_2}}{A_{M_1M_2}}\frac{m_B}{\lambda_B}\int_0^1 dx \int_0^1 dy \left[\frac{\Phi_{M_2}(x)\Phi_{M_1}(y)}{\bar{x}\,\bar{y}} + r_\chi^{M_1}\frac{\Phi_{M_2}(x)\Phi_{m_1}(y)}{x\bar{y}}\right], \tag{A6}$$

for $i = 1-4, 9, 10$,

$$H_i(M_1M_2) = -\frac{B_{M_1M_2}}{A_{M_1M_2}}\frac{m_B}{\lambda_B}\int_0^1 dx \int_0^1 dy \left[\frac{\Phi_{M_2}(x)\Phi_{M_1}(y)}{x\bar{y}} + r_\chi^{M_1}\frac{\Phi_{M_2}(x)\Phi_{m_1}(y)}{\bar{x}\,\bar{y}}\right], \tag{A7}$$

for $i = 5, 7$ and $H_i(M_1M_2) = 0$ for $i = 6, 8$ where we consider $\lambda_B = (300 \pm 100)$ MeV.

(iii) Penguin contractions [23]

The penguin contraction terms at the order of α_s can be written as

$$\begin{aligned} P_4^p(M_2) &= \frac{C_F\alpha_s}{4\pi N_c}\left\{C_1\left[\frac{4}{3}\ln\frac{m_b}{\mu} + \frac{2}{3} - G_{M_2}(s_p)\right] + C_3\left[\frac{8}{3}\ln\frac{m_b}{\mu} + \frac{4}{3} - G_{M_2}(0) - G_{M_2}(1)\right]\right\} \\ &\quad + (C_4 + C_6)\left[\frac{4n_f}{3}\ln\frac{m_b}{\mu} - (n_f - 2)G_{M_2}(0) - G_{M_2}(s_c) - G_{M_2}(1)\right] \\ &\quad - 2C_{8g^{\mathrm{eff}}}\int_0^1 \frac{dx}{1-x}\Phi_{M_2}(x), \end{aligned} \tag{A8}$$

$$P_6^p(M_2=P)=\frac{C_F\alpha_s}{4\pi N_c}\left\{C_1\left[\frac{4}{3}\ln\frac{m_b}{\mu}+\frac{2}{3}-\hat{G}_{M_2}(s_p)\right]+C_3\left[\frac{8}{3}\ln\frac{m_b}{\mu}+\frac{4}{3}-\hat{G}_{M_2}(0)-\hat{G}_{M_2}(1)\right]\right.$$
$$\left.+(C_4+C_6)\left[\frac{4n_f}{3}\ln\frac{m_b}{\mu}-(n_f-2)\hat{G}_{M_2}(0)-\hat{G}_{M_2}(s_c)-\hat{G}_{M_2}(1)\right]-2C_{8g}^{\mathrm{eff}}\right\},$$
$$P_6^p(M_2=V)=-\frac{C_F\alpha_s}{4\pi N_c}\left\{C_1[\hat{G}_{M_2}(s_p)]+C_3[\hat{G}_{M_2}(0)-\hat{G}_{M_2}(1)]\right.$$
$$\left.+(C_4+C_6)[(n_f-2)\hat{G}_{M_2}(0)+\hat{G}_{M_2}(s_c)+\hat{G}_{M_2}(1)]\right\},$$
$$P_8^p(M_2=P)=\frac{\alpha}{9\pi N_c}\left\{(C_1+N_cC_2)\left[\frac{4}{3}\ln\frac{m_b}{\mu}+\frac{2}{3}-\hat{G}_{M_2}(s_p)\right]-3C_{7\gamma}^{\mathrm{eff}}\right\},$$
$$P_8^p(M_2=V)=-\frac{\alpha}{9\pi N_c}(C_1+N_cC_2)\hat{G}_{M_2}(s_p), \tag{A9}$$

$$P_{10}^p=\frac{\alpha}{9\pi N_c}\left\{(C_1+N_cC_2)\left[\frac{4}{3}\ln\frac{m_b}{\mu}+\frac{2}{3}-G_{M_2}(s_p)\right]-3C_{7\gamma}^{\mathrm{eff}}\int_0^1\frac{dx}{1-x}\Phi_{M_2}(x)\right\}, \tag{A10}$$

where n_f the so-called number of active flavor = 5, $s_u=(\frac{m_u}{m_b})^2\approx 0$, and $s_c=(\frac{m_c}{m_b})^2$. α and α_s are EM and strong coupling constants, respectively. The functions $G_{M_2}(s)$ and $\hat{G}_{M_2}(s)$ are defined in [23].

Alongside, QCDF contain power suppressed weak annihilation contributions and the expressions are given by

(i) Annihilation contribution [23]

The annihilation contributions have the following expressions:

$$\beta_i^p(M_1M_2)=\frac{if_Bf_{M_1}f_{M_2}}{A_{M_1M_2}}b_i^p, \tag{A11}$$

where

$$b_1=\frac{C_F}{N_c^2}C_1A_1^i,\qquad b_3=\frac{C_F}{N_c^2}[C_3A_1^i+C_5(A_3^i+A_3^f)+N_cC_6A_3^3],$$
$$b_2=\frac{C_F}{N_c^2}C_2A_1^i,\qquad b_4=\frac{C_F}{N_c^2}[C_4A_1^i+C_6A_2^f],$$
$$b_{3,EW}^p=\frac{C_F}{N_c^2}[C_9A_1^i+C_7(A_3^i+A_3^f)+N_cC_8A_3^i],$$
$$b_{4,EW}^p=\frac{C_F}{N_c^2}[C_{10}A_1^i+C_8(A_2^i)]. \tag{A12}$$

The coefficients $(b_1,b_2),(b_3,b_4)$, and (b_3^{EW},b_4^{EW}) correspond to current-current, QCD penguin, and electroweak penguin annihilation contributions, respectively. Here the expressions of $A_n^{i,f}$ are given as

Case I ($M_1=M_2=P$):

$$A_1^i\approx A_2^i\approx 2\pi\alpha_s\left[9\left(X_A-4+\frac{\pi^2}{3}\right)+r_\chi^{M_1}r_\chi^{M_2}X_A^2\right],$$
$$A_3^i\approx 6\pi\alpha_s(r_\chi^{M_1}-r_\chi^{M^2})\left(X_A^2-2X^A+\frac{\pi^2}{3}\right),$$
$$A_3^f\approx 6\pi\alpha_s(r_\chi^{M_1}+r_\chi^{M^2})(2X_A^2-X_A),$$
$$A_1^f=A_2^f=0. \tag{A13}$$

Case II ($M_1 = V$, $M_2 = P$):

$$\begin{aligned} A_1^i &\approx -A_2^i \approx 6\pi\alpha_s\left[3\left(X_A - 4 + \frac{\pi^2}{3}\right) + r_\chi^{M_1} r_\chi^{M_2}(X_A^2 - 2X_A)\right], \\ A_3^i &\approx 6\pi\alpha_s\left[-3r_\chi^{M_1}\left(X_A^2 - 2X^A + \frac{\pi^2}{3} + 4\right) + r_\chi^{M_2}\left(X_A^2 - 2X_A + \frac{\pi^2}{3}\right)\right], \\ A_3^f &\approx 6\pi\alpha_s[3r_\chi^{M_1}(2X_A - 1)(2 - X_A) - r_\chi^{M_2}(2X_A^1 - X_A)], \\ A_1^f &= A_2^f = 0. \end{aligned} \tag{A14}$$

Case III ($M_1 = P, M_2 = V$):

$$\begin{aligned} A_1^i &\approx -A_2^i \approx 6\pi\alpha_s\left[3\left(X_A - 4 + \frac{\pi^2}{3}\right) + r_\chi^{M_2} r_\chi^{M_1}(X_A^2 - 2X_A)\right], \\ A_3^i &\approx 6\pi\alpha_s\left[-3r_\chi^{M_2}\left(X_A^2 - 2X^A + \frac{\pi^2}{3} + 4\right) + r_\chi^{M_1}\left(X_A^2 - 2X_A + \frac{\pi^2}{3}\right)\right], \\ A_3^f &\approx -6\pi\alpha_s[3r_\chi^{M_2}(2X_A - 1)(2 - X_A) - r_\chi^{M_1}(2X_A^1 - X_A)], \\ A_1^f &= A_2^f = 0, \end{aligned} \tag{A15}$$

where the subscripts ($n = 1, 2, 3$) and superscripts (i, f) of $A_n^{i,f}$ denote the amplitude induced from $(V - A)(V - A)$, $(V - A)(V + A)$, and $(S - P)(S + P)$ operators for former, and the gluon emission from initial and final states for later case, respectively. The chiral factor r_χ is given by

$$r_\chi^P(\mu) = \frac{2m_P^2}{m_b(\mu)(m_1 + m_2)(\mu)}, \qquad r_\chi^V(\mu) = \frac{2m_V}{m_b(\mu)}\frac{f_V^\perp(\mu)}{f_V}. \tag{A16}$$

The end point divergence that has been used can be given as

$$X_A = \ln\frac{m_B}{\Lambda_{\rm QCD}}(1 + \rho_{\rm A}\exp^{i\phi_A}), \tag{A17}$$

where $\rho_{\rm A}$ and ϕ_A can be found from [1] which is given in the below table.

Modes	$\rho_{\rm A}$	$\phi_{\rm A}$
$B_s \to PP$	1.10	−55°
$B_s \to PV$	0.85	−30°
$B_s \to VP$	0.90	−65°

[1] H.-Y. Cheng and C.-K. Chua, Phys. Rev. D **80**, 114026 (2009).
[2] J.-J. Wang, D.-T. Lin, W. Sun, Z.-J. Ji, S. Cheng, and Z.-J. Xiao, Phys. Rev. D **89**, 074046 (2014).
[3] A. Ali, G. Kramer, Y. Li, C.-D. Lu, Y.-L. Shen, W. Wang, and Y.-M. Wang, Phys. Rev. D **76**, 074018 (2007).
[4] A. R. Williamson and J. Zupan, Phys. Rev. D **74**, 014003 (2006); **74**, 03901(E) (2006).
[5] C. C. Peng *et al.* (Belle Collaboration), Phys. Rev. D **82**, 072007 (2010).
[6] T. Aaltonen *et al.* (CDF Collaboration), Phys. Rev. Lett. **106**, 181802 (2011).
[7] R. Aaij *et al.* (LHCb Collaboration), J. High Energy Phys. 10 (2012) 037.
[8] R. Aaij *et al.* (LHCb Collaboration), Phys. Rev. D **98**, 032004 (2018).
[9] R. Aaij *et al.* (LHCb Collaboration), J. High Energy Phys. 10 (2013) 183.
[10] Y. Amhis *et al.* (HFLAV Collaboration), Eur. Phys. J. C **77**, 895 (2017).
[11] M. Tanabashi *et al.* (Particle Data Group), Phys. Rev. D **98**, 030001 (2018).
[12] T. Aaltonen *et al.* (CDF Collaboration), Phys. Rev. Lett. **102**, 201801 (2009).
[13] R. Aaij *et al.* (LHCb Collaboration), Phys. Rev. Lett. **118**, 251802 (2017).
[14] C. Bobeth, M. Gorbahn, T. Hermann, M. Misiak, E. Stamou, and M. Steinhauser, Phys. Rev. Lett. **112**, 101801 (2014).
[15] Y. Li, W.-L. Wang, D.-S. Du, Z.-H. Li, and H.-X. Xu, Eur. Phys. J. C **75**, 328 (2015).
[16] R. Mohanta and A. K. Giri, Phys. Rev. D **79**, 057902 (2009).

[17] C.-W. Chiang, N. G. Deshpande, and J. Jiang, J. High Energy Phys. 08 (2006) 075.
[18] B. Mawlong, R. Mohanta, and A. K. Giri, Phys. Lett. B **668**, 116 (2008).
[19] G. Barenboim, F. J. Botella, and O. Vives, Phys. Rev. D **64**, 015007 (2001).
[20] D. Atwood and G. Hiller, arXiv:hep-ph/0307251.
[21] A. K. Giri and R. Mohanta, Phys. Rev. D **68**, 014020 (2003).
[22] G. Buchalla, A. J. Buras, and M. E. Lautenbacher, Rev. Mod. Phys. **68**, 1125 (1996).
[23] M. Beneke and M. Neubert, Nucl. Phys. **B675**, 333 (2003).
[24] A. Hayakawa, Y. Shimizu, M. Tanimoto, and K. Yamamoto, Prog. Theor. Exp. Phys. **2014**, 23B04 (2014).
[25] S. Descotes-Genon and P. Koppenburg, Annu. Rev. Nucl. Part. Sci. **67**, 97 (2017).
[26] N. de Groot, W. N. Cottingham, and I. B. Whittingham, Phys. Rev. D **68**, 113005 (2003).
[27] M. Beneke, T. Feldmann, and D. Seidel, Eur. Phys. J. C **41**, 173 (2005).
[28] S. Sahoo and R. Mohanta, J. Phys. G **44**, 035001 (2017).
[29] R. Mohanta, Phys. Rev. D **71**, 114013 (2005).
[30] A. Khodjamirian and A. V. Rusov, J. High Energy Phys. 08 (2017) 112.
[31] Q. Chang, X.-Q. Li, and Y.-D. Yang, J. High Energy Phys. 02 (2010) 082.
[32] V. Barger, L. L. Everett, J. Jiang, P. Langacker, T. Liu, and C. E. M. Wagner, J. High Energy Phys. 12 (2009) 048.
[33] P. Langacker and M. Plumacher, Phys. Rev. D **62**, 013006 (2000).
[34] X.-G. He and G. Valencia, Phys. Rev. D **74**, 013011 (2006).
[35] S. Baek, J. H. Jeon, and C. S. Kim, Phys. Lett. B **664**, 84 (2008).
[36] L. L. Everett, J. Jiang, P. G. Langacker, and T. Liu, Phys. Rev. D **82**, 094024 (2010).
[37] V. Barger, C.-W. Chiang, J. Jiang, and P. Langacker, Phys. Lett. B **596**, 229 (2004).
[38] C.-H. Chen, C.-Q. Geng, and W. Wang, J. High Energy Phys. 11 (2010) 089.
[39] N. G. Deshpande and D. K. Ghosh, Phys. Lett. B **593**, 135 (2004).
[40] R. Mohanta and A. K. Giri, Phys. Rev. D **78**, 116002 (2008).
[41] C.-D. Lü, Y.-L. Shen, Y.-M. Wang, and Y.-B. Wei, J. High Energy Phys. 01 (2019) 024.
[42] C. M. Bouchard, G. P. Lepage, C. Monahan, H. Na, and J. Shigemitsu, Phys. Rev. D **90**, 054506 (2014).
[43] H. Na, C. J. Monahan, C. T. H. Davies, R. Horgan, G. P. Lepage, and J. Shigemitsu, Phys. Rev. D **86**, 034506 (2012).
[44] K. A. Olive *et al.* (Particle Data Group), Chin. Phys. C **38**, 090001 (2014).